Do loading path and specimen thickness affect the brittle compressive failure of ice?

A.L. FORTT, E.M. SCHULSON

Thayer School of Engineering, Dartmouth College, Hanover, New Hampshire 03755-8000, USA
E-mail: andrew.l.fortt@dartmouth.edu

ABSTRACT. Compressive experiments were performed on square (160 mm × 160 mm) prismatic specimens of columnar-grained, S2 freshwater ice, biaxially loaded across the columns at –10°C. The work focused on brittle behavior, achieved by deforming the specimens at an applied strain rate of $4.5 \pm 1.2 \times 10^{-3}\,s^{-1}$ in the direction of shortening. The results show that the specimen thickness (25–150 mm) has no detectable effect on the terminal failure strength of the ice. Likewise, the strength of the ice when loaded under proportional loading, where the minor stress varies during the test, was similar to that when loaded under a constant minor stress, implying that terminal failure depends only on the stress state and not on the path taken.

1. INTRODUCTION

Here we present terminal failure data obtained from the across-column biaxial compression of columnar-grained S2 ice loaded using two procedures. The first procedure, termed proportional loading, has been used in previous investigations (e.g. Iliescu and Schulson, 2004). We use it here to investigate whether specimen thickness affects failure under low confinement where Coulombic shear faulting limits the compressive strength (Iliescu and Schulson, 2004). In this procedure the minor stress, σ_{22}, is applied in direct proportion to the major stress, σ_{11}, such that the stress ratio $R = \sigma_{22}/\sigma_{11}$ defines the loading path in principal stress space. The second procedure, termed the constant minor stress procedure, simply applies a constant minor stress, σ_{22}, throughout the experiment. The question is whether the loading path affects the failure stress. The question is an important one, because it bears on the issue of terminal failure and whether the failure stress depends only on the stress ratio at failure or also on the path taken to get there. We also consider whether specimen thickness affects the failure stress. The work follows from earlier studies on the strength of columnar-grained S2 ice. In that work the material was brought to terminal failure using either proportional loading (Frederking, 1977; Timco and Frederking, 1986; Richter-Menge, 1991; Smith and Schulson, 1993; Schulson and Nickolayev, 1995; Iliescu and Schulson, 2004) or constant confinement (Sammonds and others, 1998).

2. EXPERIMENTAL PROCEDURE

Biaxial compression experiments were performed on square prismatic specimens of freshwater columnar S2 ice, harvested from 200 mm thick sheets grown in the laboratory using the procedure described by Smith and Schulson (1993).

The ice was transparent and free from both cracks and visible air inclusions. Its density at –10°C was $916.0 \pm 5.2\,kg\,m^{-3}$, in close agreement with reported values of fully dense freshwater ice (Hobbs, 1974). The mean column diameter was 5–6 mm. The crystallographic *c* axes were perpendicular within ±8° to the longitudinal axes of the columnar grains, but randomly orientated within this plane. Thus, the material can be classified as S2 ice (Michel and Ramseier, 1971).

Square prismatic specimens (160 mm × 160 mm) were prepared from roughly cut blocks using a horizontal milling machine. Opposing specimen faces were machined parallel, to a tolerance of ±0.05 mm. Four thicknesses (dimension X_3 in Fig. 1b) were used: ~25, ~50, ~75 and ~150 mm. In the constant minor stress tests the thickness was constant at ~50 mm. The specimens were prepared with the long axes of the columnar-shaped grains perpendicular to the largest faces, as shown in Figure 1a.

In both loading procedures biaxial compressive loads were applied across the long axis of the columnar-shaped grains (Fig. 1b), using a multiaxial servohydraulic testing system (MATS) and polished brass platens placed on the MATS loading platens. A strain rate of $\dot{\varepsilon}_{11} = (4.5 \pm 1.2) \times 10^{-3}\,s^{-1}$ was applied along the direction of shortening. Terminal failure generally occurred at a strain of $\varepsilon_{11} = (4.2 \pm 1.1) \times 10^{-3}$. In all tests the ice was equilibrated at -10.0 ± 0.2°C.

Proportional-loading procedure

In this procedure the horizontal axis of the MATS was programmed to control a set proportion of the load produced by the vertical actuators. The proportion was set to be a constant for the duration of each test, but varied slightly, typically by $\Delta R \sim \pm 0.03$. The proportion was measured at the time at which the maximum stress occurred. Tests were performed over the range $0.02 < R < 0.14$. The loading history is shown schematically in Figure 2. With reference to that figure:

(a) The specimen was placed on the lower platen of the MATS and the pair of major (vertical) actuators was slowly brought into contact with the specimen. The load was kept small (~0.03 MPa) to allow the horizontal actuators to reorient the specimen as needed, for uniform contact along the loading faces.

(b) The pair of minor (horizontal) actuators was slowly brought into contact with the specimen until a small load (~0.03 MPa) was applied.

(c) and (d) The major load followed by the minor load was increased slightly (to ~0.15 MPa) and the specimen was allowed to creep seat. A time of ~10 min was used, as this has previously been found to yield reproducible results.

https://doi.org/10.3189/172756507782202838 Published online by Cambridge University Press

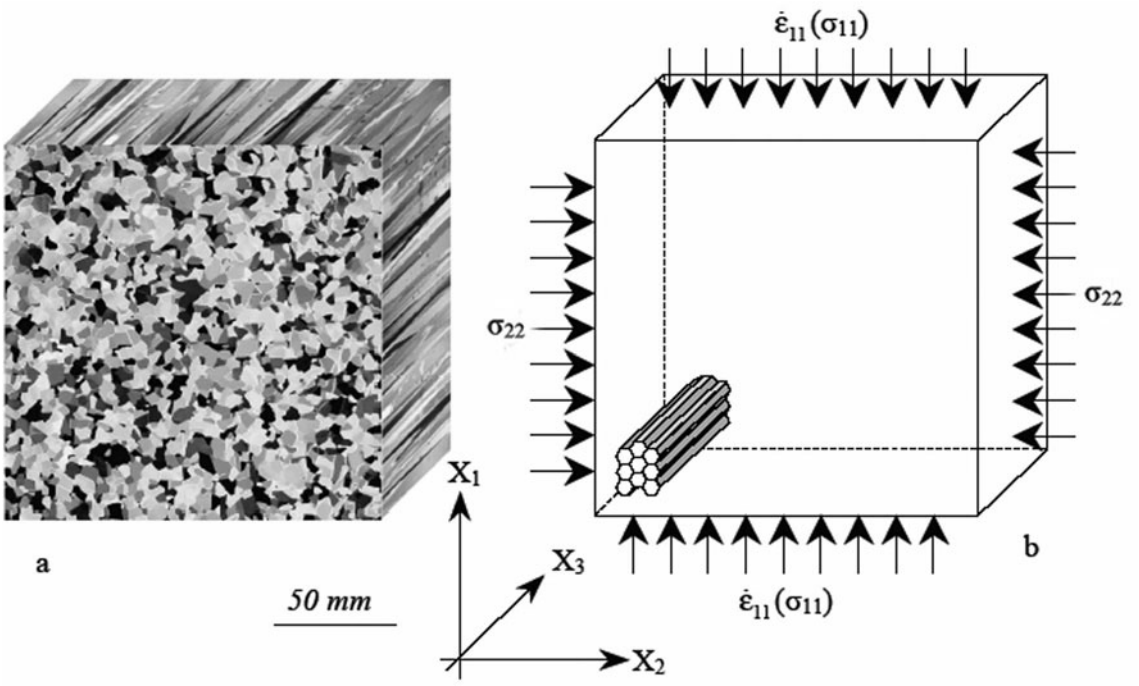

Fig. 1. (a) Composite polarized photograph of laboratory-grown freshwater ice specimen microstructure. (b) Schematic representation of loading stage. In the proportional-loading procedure $\sigma_{22} = R\sigma_{11}$. In the constant minor stress procedure σ_{22} is constant.

(e) The minor load was adjusted to give the desired proportion between the major and minor loads.

(f) Once the test began, the controller instructed the major actuators to move at a given displacement rate until a given displacement was reached, during which period the load increased linearly with time until dropping suddenly on formation of a fault.

Constant minor stress procedure

In this procedure the pair of minor actuators was programmed to maintain a constant stress, σ_{22}, on the specimen (Fig. 1b), independent of the vertical stress. The stress level was held constant during each test, but was varied between tests, $0.15 \leq \sigma_{22} \leq 3.07$ MPa. Under higher minor stresses testing became unsafe: on failure the horizontal actuators continued to try to apply the programmed value of σ_{22}; in doing so they would move quickly in, crush the specimen and possibly damage the actuator platens. (This was not a limitation in proportional loading; in that procedure when the vertical load dropped to zero on failure so did the horizontal load and the horizontal actuators backed off.) The loading history is shown schematically in Figure 2. With reference to that figure:

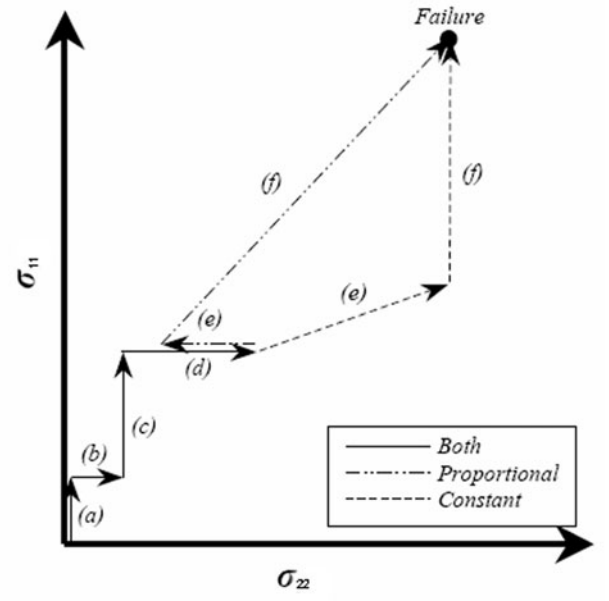

Fig. 2. The σ_{11}–σ_{22} loading path for the proportional-loading and constant minor stress procedures.

(a–d) The initial loading was identical to that of the proportional-loading procedure.

(e) The pair of major actuators was switched to stroke control, locking them in place. The load on the minor horizontal actuators was adjusted until the desired level was reached. Due to the major actuators being locked in place, the load on them would decrease or increase, in approximate proportion to Poisson's ratio.

(f) The pair of major actuators was again instructed to maintain a given displacement rate, until a given displacement was reached. Concurrently, the pair of minor actuators was instructed to maintain a constant load, independent of the load from the vertical actuators.

3. RESULTS

Specimen thickness

Figure 3a shows a typical stress–time curve for the proportional-loading procedure. We define the terminal failure stress as the highest stress recorded during the test. In every experiment the ice failed through the formation of either a single Coulombic fault or a pair of conjugate Coulombic faults (Fig. 3c), as found earlier (Iliescu and

https://doi.org/10.3189/172756507782202838 Published online by Cambridge University Press

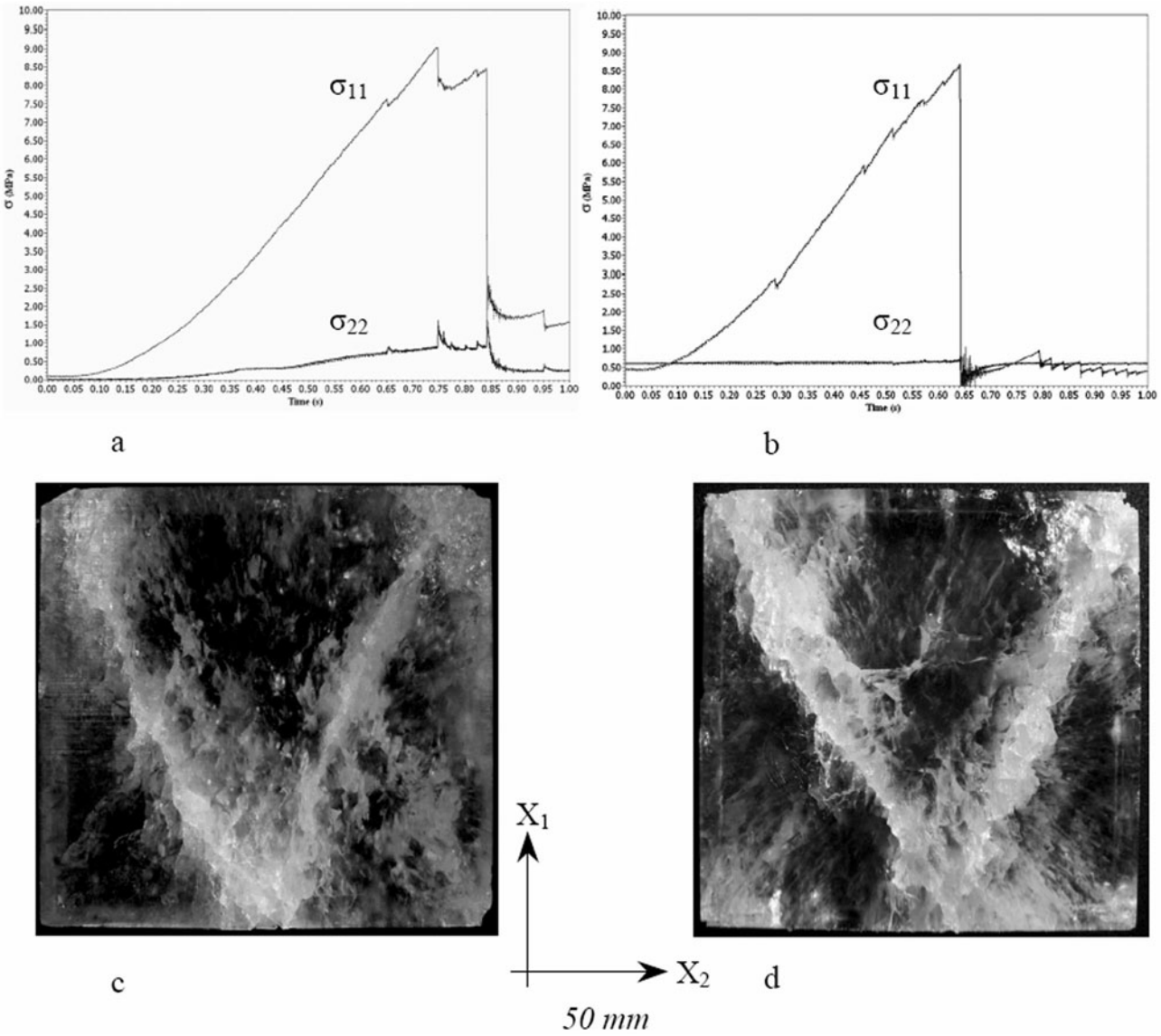

Fig. 3. (a, b) Stress–time curves from (a) a proportionally loaded test and (b) a constant minor stress test. (c, d) Photographs of a faulted specimen ($X_3 = \sim 50$ mm) showing conjugate faults from (c) a test performed under proportional loading, corresponding to the stress–time curve in (a), and (d) a test performed under constant minor stress, corresponding to the stress–time curve in (b).

Schulson, 2004). Figure 4a–c show the terminal failure stresses obtained from each test, separated into bins according to the four specimen thicknesses (~25, ~50, ~75 and ~150 mm). From Figure 4d it can be seen that all the data are confined within the same band of scatter. Table 1 lists the slope, intercept and correlation coefficient, obtained by applying a linear trend to the data in each bin. There appears to be no systematic effect of thickness on either the slope or the intercept. We conclude therefore that, over the range explored, specimen thickness has no significant effect on the brittle failure stress of S2 columnar-grained ice biaxially loaded under moderate confinement across the columns. This conclusion is in agreement with previous findings on the brittle compressive strength of granular ice (Kuehn and others, 1993) loaded uniaxially.

Loading path

Figure 3b shows a typical stress–time curve for a constant minor stress test. Note that σ_{22} is constant. Again, terminal failure was marked by the formation of either a single Coulombic shear fault or a pair of conjugate Coulombic shear faults over the range of σ_{22} investigated. An example is shown in Figure 3d. The faults were identical in appearance to those formed in specimens that were proportionally loaded. Figure 5 compares terminal failure strengths obtained using the constant minor stress procedure with those obtained using the proportional-loading procedure. To avoid confusion we show only the limits of the band of data shown in Figure 4d, but show the full set of data obtained by Iliescu and Schulson (2004). The results indicate that there is no detectable effect of loading path on the strength of the ice.

4. DISCUSSION

It is not surprising that the specimen thickness has an insignificant effect on the compressive strength (beyond that where buckling limits failure). When loaded across the columns, S2 ice exhibits essentially plane-strain inelastic deformation within the X_1-X_2 plane (defined in Fig. 1a), and

https://doi.org/10.3189/172756507782202838 Published online by Cambridge University Press

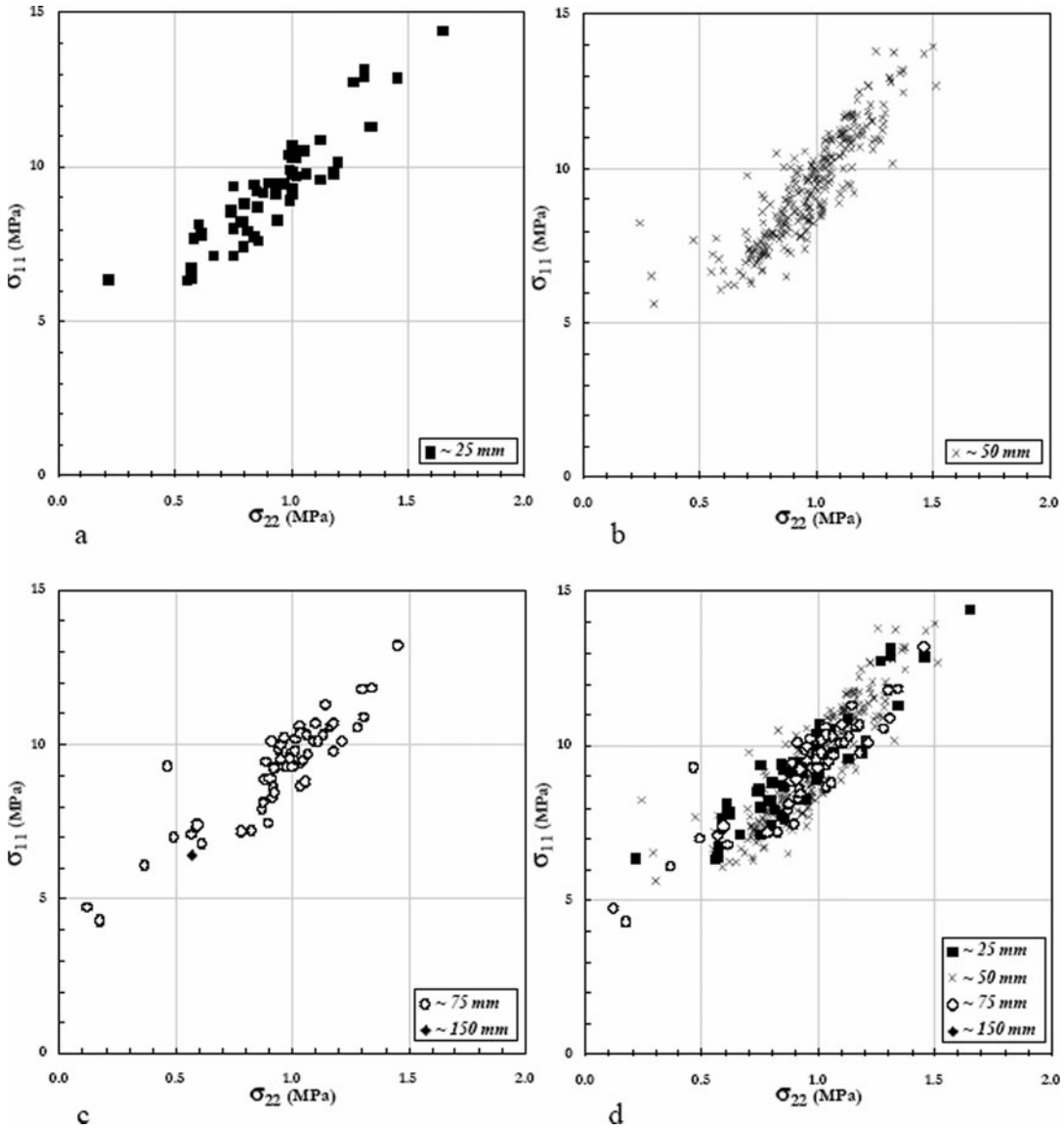

Fig. 4. Failure stresses obtained using the proportional-loading procedure, grouped according to specimen thickness. All specimens possessed dimensions of $X_1 = X_2 = \sim 160$ mm. The value listed in the legend is that for the thickness. Note the different scales on the abscissa and ordinate. (a) $X_3 = \sim 25$ mm; (b) $X_3 = \sim 50$ mm; (c) $X_3 = \sim 75$ mm; and (d) $X_3 = \sim 150$ mm. All data grouped together.

so the thickness is not an important factor. Along any direction within that plane, there were enough grains (>16) to constitute polycrystalline behavior under across-column loading. Cracks nucleate on planes parallel to the no-load direction, and then lengthen somewhat along the direction of shortening, eventually linking up to form the Coulombic fault (Schulson and others, 1999).

Table 1. Parametric values obtained from applying a linear trend to the data in each thickness bin and combining all the data (Σ)

Specimen thickness, X_3	Slope	Intercept	Correlation coefficient, r^2
mm		MPa	
~25	6.40	3.36	0.83
~50	7.59	2.05	0.77
~75	5.64	3.90	0.82
~150	–	–	–
Σ	6.92	2.73	0.77

Turning to the observed path independence of terminal failure, this implies that the brittle compressive strength of S2 ice under low minor stresses depends only on the stress state at terminal failure, and not on the path taken to get there. This result is gratifying in that it is in keeping with current theory of brittle compressive failure (Renshaw and Schulson, 2001). It suggests that the evolution of damage that eventually interacts to trigger faulting is also independent of the path taken. We did not perform detailed microstructural examinations such as those performed by Schulson and others (1999) and cannot say with certainty that this is true. However, if the evolution does depend on the path, then we expect the dependence to be relatively small.

Finally, the results of the present experiments strengthen earlier results of path independence (Schulson and Iliescu, 2006). There we asked whether terminal failure of S2 under proportional across-column straining occurred through a different process than under proportional loading; we found

https://doi.org/10.3189/172756507782202838 Published online by Cambridge University Press

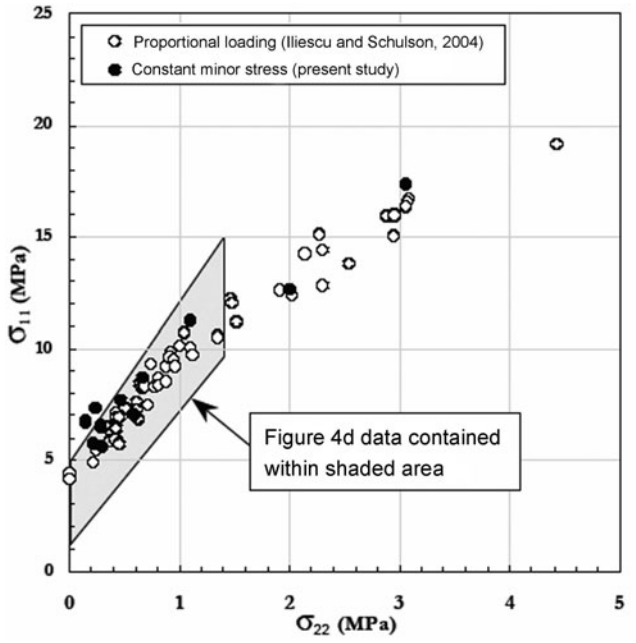

Fig. 5. Comparison of failure stresses obtained using the proportional-loading and constant minor stress procedures. Note the different scales on the abscissa and ordinate.

that it did not. Along both paths, the failure mode and failure stress were indistinguishable.

How general are the current findings? Although strictly only applicable to freshwater S2 columnar ice loaded within the regime of brittle behavior, we expect they also apply to granular ice triaxially loaded under moderate confinement. We base that expectation on the observation by Weiss and Schulson (1995) that the low-confinement triaxial strength of granular ice determined through proportional loading was similar to that obtained by Jones (1982) and by Rist and Murrell (1994) under constant confining pressure. Our sense, therefore, is that, in general, the brittle compressive failure of ice loaded under confinement sufficiently low that Coulombic faulting limits strength depends only on the stress state at terminal failure, independent of the loading path through which that state is reached.

5. CONCLUSIONS

In conclusion, results from biaxial compression experiments at –10°C on laboratory-grown freshwater S2 columnar ice, biaxially loaded across the columns at an applied strain rate sufficiently high to impart brittle behavior ($\dot{\varepsilon}_{11} = 4.5 \times 10^{-3}\,s^{-1}$) show that specimen thickness (over the range 25–150 mm) has no detectable effect on the brittle compressive strength. Similarly, the strength of the ice obtained when loaded under proportional loading is indistinguishable from that obtained when loaded under a constant minor stress.

ACKNOWLEDGEMENTS

We acknowledge the thoughtful comments of the editor S. Jones and of the anonymous reviewers. This work was supported by the US National Science Foundation (grant Nos. OPP-0328605 and ARC-0520375) and the US National Oceanic and Atmospheric Administration (grant No. NA17RP1400).

REFERENCES

Frederking, R. 1977. Plane-strain compressive strength of columnar-grained and granular-snow ice. *J. Glaciol.,* **18**(80), 505–516.

Hobbs, P.V. 1974. *Ice physics.* Oxford, Clarendon Press.

Iliescu, D. and E.M. Schulson. 2004. The brittle compressive failure of fresh-water columnar ice loaded biaxially. *Acta Mater.,* **52**(20), 5723–5735.

Jones, S.J. 1982. The confined compressive strength of polycrystalline ice. *J. Glaciol.,* **28**(98), 171–177.

Kuehn, G.A., E.M. Schulson, D.E. Jones and J. Zhang. 1993. The compressive strength of ice cubes of different sizes. *J. Offshore Mech. Arct. Eng. ASME,* **12**, 142–148.

Michel, B. and R.O. Ramseier. 1971. Classification of river and lake ice. *Can. Geotech. J.,* **8**(1), 36–45.

Renshaw, C.E. and E.M. Schulson. 2001. Universal behaviour in compressive failure of brittle materials. *Nature,* **412**(6850), 897–900.

Richter-Menge, J.A. 1991. Confined compressive strength of horizontal first-year sea ice samples. *J. Offshore Mech. Arct. Eng. ASME,* **113**, 344–351.

Rist, M.A. and S.A.F. Murrell. 1994. Ice triaxial deformation and fracture. *J. Glaciol.,* **40**(135), 305–318.

Sammonds, P.R., S.A.F. Murrell and M.A. Rist. 1998. Fracture of multiyear sea ice. *J. Geophys. Res.,* **103**(C10), 21,795–21,815.

Schulson, E.M. and D. Iliescu. 2006. Brittle compressive failure of ice: proportional straining vs. proportional loading. *J. Glaciol.,* **52**(177), 248–250.

Schulson, E.M. and O.Y. Nickolayev. 1995. Failure of columnar saline ice under biaxial compression: failure envelopes and the brittle-to-ductile transition. *J. Geophys. Res.,* **100**(B11), 22,383–22,400.

Schulson, E.M., D. Iliescu and C.E. Renshaw. 1999. On the initiation of shear faults during brittle compressive failure: a new mechanism. *J. Geophys. Res.,* **104**(B1), 695–705.

Smith, T.R. and E.M. Schulson. 1993. The brittle compressive failure of fresh-water columnar ice under biaxial loading. *Acta Metall. Mater.,* **41**(1), 153–163.

Timco, G.W. and R.M.W. Frederking. 1986. Confined compression tests: outlining the failure envelope of columnar sea ice. *Cold Reg. Sci. Technol.,* **12**(1), 13–28.

Weiss, J. and E.M. Schulson. 1995. The failure of fresh-water granular ice under multiaxial compressive loading. *Acta Metall. Mater.,* **43**(6), 2303–2315.

MS received 10 October 2006 and accepted in revised form 20 January 2007